

Classification of Orbits with Regard to Collision Hazard in Space

V.A. Chobotov*

The Aerospace Corporation, El Segundo, California

The presence of some 5000 tracked objects in orbit and the presumed existence of a significantly greater population of smaller objects constitute a real and increasing collision hazard for present and future missions in space. The study considers the distribution of the tracked population as function of altitude and orbital inclination. Sample encounter parameters (number, miss distance, and relative velocity) are generated by simulation and used to classify low-altitude and geostationary orbits in accordance with the degree of collision hazard presented. Application of the technique is made to representative Space Shuttle and geosynchronous orbit missions. It is found that the collision hazard is generally a nonuniform function of orbital inclination and longitudinal location in geosynchronous orbit.

Nomenclature

A_{MAX}	= projected area of encounter sphere = πR_{MAX}^2
A_S	= projected area of spacecraft, = πR_S^2
F	= flux of objects relative to spacecraft in orbit
h	= spacecraft orbit altitude
i	= spacecraft orbit inclination
N_T	= total encounters
R	= radius of spacecraft orbit
R_S	= effective collision radius of spacecraft
R_{MIN}	= distance of closest approach
R_{MAX}	= radius of encounter sphere
V_S	= orbital velocity of spacecraft
V_O	= orbital velocity of object
V_R	= relative velocity at closest approach
θ	= relative (aspect) angle at closest approach

Introduction

THE presence of manmade debris in space presents a collision hazard to spacecraft which is proportional to the density of debris, relative velocity at encounter, projected area of the spacecraft, and mission duration. The hazard is from two populations: 1) Large objects which can be tracked by radar and are in the vicinity of operational orbits. These objects consist mostly of explosion fragments, but include spent spacecraft, rocket stages, and payload separation devices. Objects larger than 4 cm diameter fall into this category. 2) Smaller objects which cannot be tracked but are presumed to exist as a result of more than 70 spacecraft explosions to date. The existence of this population can be inferred from terrestrial tests in which the particle distributions from high- and low-intensity explosions have been measured. The number of such particles may be in the tens of thousands or even in the millions. Several studies¹⁻⁶ have examined the origin and distribution of the tracked population of objects and implications for future missions. This study considers the distribution of the tracked population of objects as a function of altitude and orbital inclination. Representative encounter parameters such as the number, relative velocity, and miss distance are determined for circular mission orbits and are used to classify regions of space according to the degree of collision hazard presented.

Implications for Space Shuttle and geosynchronous orbits are examined.

Low and Intermediate Altitude Orbits

A numerical simulation has been used to examine the encounter parameters between a spacecraft of radius R_S in a given circular orbit and a population of objects from the March 1981 NORAD catalog. The encounter parameters include the distance of closest approach R_{MIN} , relative velocity V_R , the aspect angle θ , and the number of encounters N per revolution of the spacecraft orbit within the spacecraft-centered encounter sphere of radius R_{MAX} . Circular low and intermediate altitude spacecraft orbits were considered (500-2000 km altitude) for inclinations of 0, 45, 90, and 135 deg. Typical orbital and encounter geometries are illustrated in Figs. 1 and 2, respectively.

In analogy with the kinetic model of a gas, the positions of the objects within the encounter sphere can be assumed to be randomly distributed and moving in a straight line. This assumption is valid for $R_{MAX} \ll R$ where R is the radius of the spacecraft orbit. The number of encounters per unit time per unit area (such as the projected area of the encounter sphere A_{MAX}) is the flux F . The probability of encountering an object by the projected area of the spacecraft (or a collision) is then given by

$$p(\text{col}) = 1 - e^{-FA_S \Delta t} \approx FA_S \Delta t \quad \text{if } < 0.1 \quad (1)$$

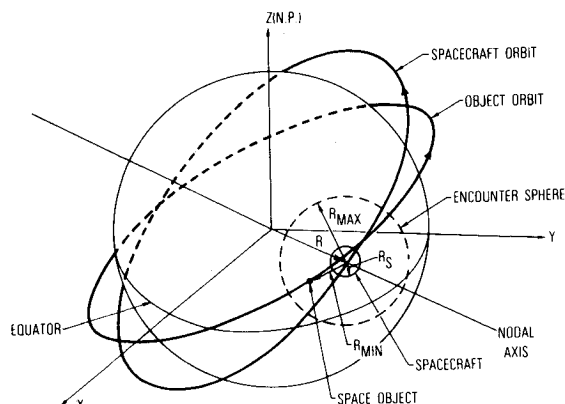


Fig. 1 Orbital geometry.

Submitted Sept. 22, 1982; revision received March 7, 1983. Copyright © American Institute of Aeronautics and Astronautics, Inc., 1983. All rights reserved.

*Manager, Space Hazards Office, Astrodynamics Department.

The flux F has been determined as a function of R_{MAX} within a 300 km radius in 20 km steps per orbital revolution of the spacecraft. The spatial distribution of F with R_{MAX} was generally found to be nonuniform and in some cases

significantly higher (e.g., up to a factor of 2 or more) for lower R_{MAX} . Nevertheless, the results (plotted in Fig. 3) are representative for the cases examined. The flux (and hence the probability of collision) is seen to be maximum in the 600-1200 km altitude range. It is also greater for higher inclination orbits.

The mean relative velocity \bar{V}_R and the mean aspect angle $\bar{\theta}$ are given in Figs. 4 and 5, respectively, as a function of altitude with the inclination angle i as a parameter. It can be seen that \bar{V}_R is of the order of 11 km/s with some variations at lower altitude (8-10 km/s) and for equatorial ($i=0$ deg) orbits. The mean aspect angle (relative angle at encounter) is of the order of 90 deg, indicating that the space objects tend to encounter the spacecraft in a cross-track direction.

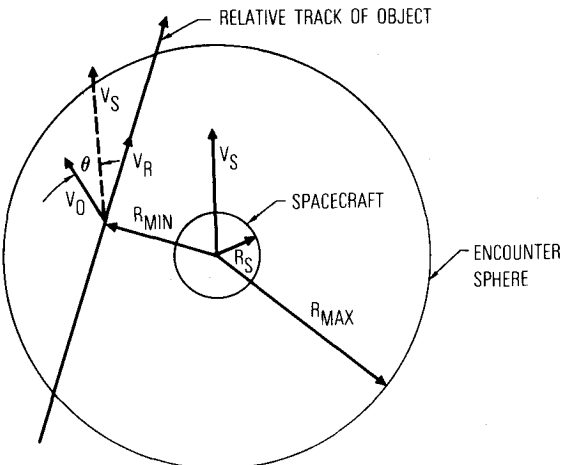


Fig. 2 Encounter geometry.

Table 1 Shuttle encounters within 200 km of NORAD catalog objects at 278 km altitude

	Two days			Four days		
Shuttle orbit inclination i , deg	28.5	57	98	28.5	57	98
N_T	35	44	56	67	79	108
R_{MIN} , km	138	150	145	142	146	147
\bar{V}_R , km/s	9.37	10.7	12.5	9.45	10.8	12.4
Element sets used	33	35	37	46	47	50

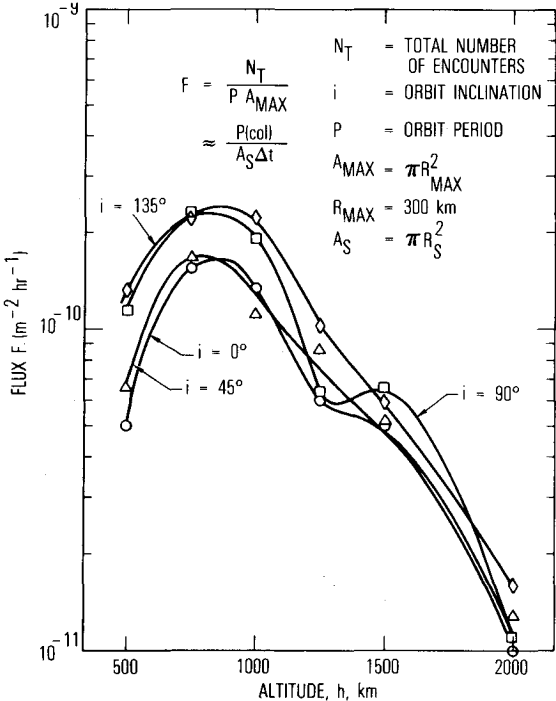


Fig. 3 Flux rate vs altitude.

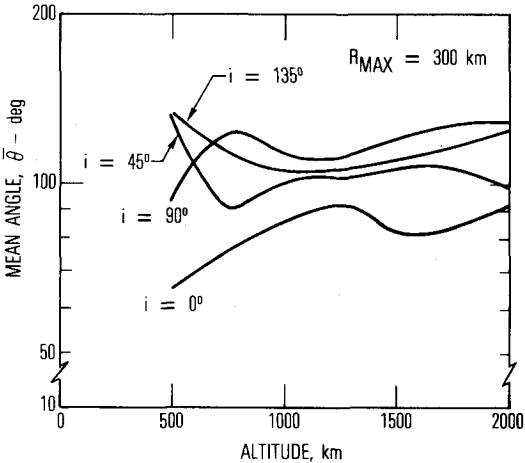


Fig. 5 Mean relative angle at encounter.

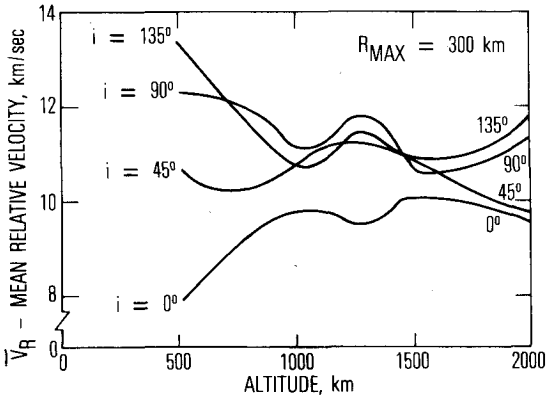


Fig. 4 Mean relative velocity at encounter.

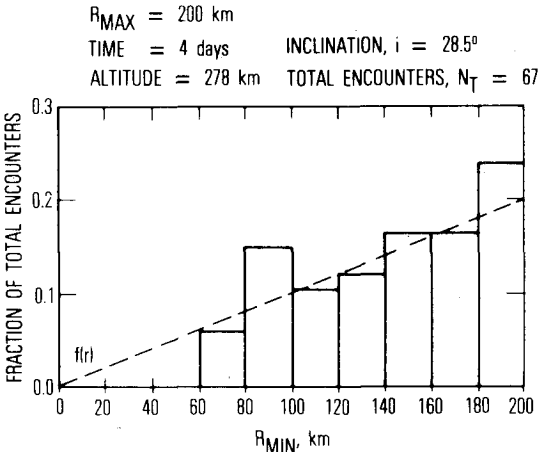


Fig. 6 Normalized encounter frequency distribution for a Shuttle orbit.

Table 2 Geostationary satellites—NORAD catalog for September 1981-January 1982
(± 2 deg of nominal longitude)

1. Meteosat 2	33. OPS 9441	65. Intelsat 4AF4
2. INTELSAT 4F2	34. GOES D	66. Intelsat V Fl
3. OTS-2	36. OPS 9443	67. OPS 6393
4. 12618	37. OPS 2112	68. Intelsat 4AF2
5. Raduga 6	40. 12309	69. NATO 3B OPS 9364
7. 83501	41. WESTAR	70. 80021
8. Gorizont 3	42. RCA B	71. NATO 3B OPS 9363
9. 83019	43. Ekran 7	72. Marisat A
11. OPS 9434	44. Anik 3 (Telesat C)	73. Gorizont A
12. Intelsat 4AF6	46. Anik 4	74. OPS 9444
13. OPS 9442	48. GOES B	75. Symphonie A
15. OPS 3151	49. LES 9	
16. Marisat B	50. ATS 3	
17. OPS 6392	51. 83535	6. GEOS 2 ^a
18. OPS 3811	52. Anik 1 (Telesat)	10. POS Ekran 1 ^a
19. 83018	53. NATO I OPS 9361	14. Intelsat 3 F3 ^a
21. Intelsat 4AF3	54. 12065	20. Raduga 4 ^a
22. Ekran 5	55. OPS 6391	23. Ekran 6 ^a
24. UNK	56. Westar A	35. SMS C (GOES A) ^a
25. 12046 Fltsatcom-D	57. Comstar 1 D2	38. OPS 7484 ^a
26. OPS 9438	58. Comstar 1 D1	39. RCA A ^a
27. Intelsat 4F8	59. Westar C	45. NATO 2 ^a
28. Marisat C	60. COMSTAR 1 D3	47. LES 8 ^a
29. Intelsat 4F4	61. GOES E	
30. Intelsat 4F7	62. 83561	
31. ATS 1	63. ATS 5	
32. OPS 3151 R/B	64. Intelsat 4F3	

^a ± 3.5 deg of nominal longitude.

Table 3 Listing of drifting geosynchronous satellites (September 1981-January 1982)

$D^a < 10.11$	$10.11 < D \leq 11.01$	$11 < D \leq 151$	$151 < D$
3. Meteosat	2. OPS 3165	1. 83586	8. Symphonie B
14. Cosmos 775	7. Raduga 1 R/B	4. Ekran 2 R/B	10. Elektron 4 R/B
	9. Molniya 1S		
40. Raduga 5	16. Palapa B	5. 83005	26. Elektron 4
44. BSE	20. UNK	6. 83506	28. OPS 9431-2 R/B
46. CS	23. Gorizont	11. Ekran 6 R/B	29. OPS 9431 9432 R/B
56. GMS	24. Ekran 4	12. 83858	33. 11728 ECS B R/B
57. OPS 9437	27. Raduga 7	13. Gorizont 3 R/B	34. 83599
68. 12677	30. UNK	15. OPS 6157 R/B	35. OPS 9441-2 R/B
89. 83539	31. 08513	17. ECS B	38. 03292
91. OPS 9431	32. UNK	18. 12897	39. IDCSP 20-27 R/B
93. 83502	36. Ekran 3	19. Cosmos 637	43. UNK
97. 83584	45. 12545	21. Raduga 8	49. UNK
101. UNK	47. UNK	22. OPS 2112 R/B	52. LES 8,9/SOL 11A,B R/B
106. 83017	48. Palapa A	25. 83025	59. OPS 5960
111. 83595	50. Gorizont 2	37. ATS F R/B	61. 83571
113. Raduga 3	51. 83572	41. Transtage	62. SMS A
120. 12339	53. Skynet 2B OPS 9354	42. LES 6 R/B	63. Raduga 6 R/B
122. Intelsat 1F1	58. ETS 2	54. Ekran	64. OPS 9347 (IDSCS 26)
125. Nato 3 C OPS 9365	60. OPS 3165 R/B	55. UNK Lost	66. OPS 9326 (IDCSP 13)
133. Intelsat 4A F1	72. Intelsat 4F5	65. 12855	67. Gorizont 4 R/B
139. Intelsat 4 F1	75. UNK	69. COSMOS 637 R/B	73. 04478
	77. Raduga 2	70. OPS 1570	78. OPS 9443/9444 R/B
	81. OPS 9433	71. 80277	82. OPS 9433/9434 R/B
	84. UNK	74. Ekran 1 R/B	83. 06976
	85. OPS 9432	76. Ekran 2	104. 83574
	87. GOES C	79. Gorizont 1 R/B	110. 83585
	88. 83590	80. OPS 3811 R/B	114. Raduga 3 R/B
	95. LES 6	86. OPS 7484 R/B	115. OPS 9437/9438 R/B
	100. UNK	90. OV2-5	117. 02222
	102. Sirio	92. UNK Lost	118. IDCSP 1-7 R/B
	103. UNK	94. OPS 1570 DEB	119. 83589
	105. Cosmos 775 R/B	96. OPS 1570 R/B	121. ECS
	107. Anik 2	98. 12371	124. OPS 5960 R/B
	108. 12635	99. 83853	126. Elektron 1-2 R/B
	109. CTS A	112. Skynet A	128. INTELSAT 3 F8
	116. SMS B	127. 80133	129. Elektron 2
	123. IUE	130. Scatha	132. EQS 2
	140. 83013	131. OPS 6157	134. 02868
	142. 12089	136. 83587	135. IDCSP 17-19 R/B
			137. Raduga 4 R/B
			138. Raduga 4 R/B
			141. Raduga 7 R/B
			143. ATS F

^a D = drift rate (deg/day).

Table 4 Predicted worst case encounters for four geosynchronous satellites

Satellite 1	Satellite 2	R_{MIN} , km	Date	Satellites time, GMT
10669/6391 (100°W)	12065/SBS-A	2.6	23 Jul 81	2305
	12065/SBS-A	4.2	29 Jul 81	2220
	12065/SBS-A	5.6	02 Aug 81	0952
	12065/SBS-A	4.0	03 Aug 81	0943
	3431/LES 6	45.0	31 Aug 81	1032
	10953/GOES-C	31.0	16 Nov 81	0501
	8585/CTS-A	48.0	23 Nov 81	1849
	4353/NATO 1	28.0	13 Dec 81	0413
	12065/SBS-A	6.0	19 Dec 81	2341
	12065/SBS-A	17.9	22 Dec 81	2257
	12065/SBS-A	14.0	25 Dec 81	2302
	12065/SBS-A	8.5	27 Dec 81	2306
	4353/NATO	5.2	04 Jan 82	0248
	1940/RB	36.0	11 Jul 81	2019
10001/9438 (175°E)	7544/INTELSAT 4F8	15.0	14 Sep 81	0911
	80277/UNKNOWN	14.0	22 Sep 82	1508
	11436/RB	36.0	14 Oct 81	0629
	11684/RB	26.0	21 Oct 81	0512
	9478/MARISAT-C	2.9	02 Nov 81	2346
	9478/MARISAT-C	10.3	03 Nov 81	2346
	8978/MARISAT-C	5.8	07 Nov 81	2326
	9478/MARISAT-C	3.7	07 Nov 81	2346
	6796/INTELSAT 4-F7	4.0	18 Dec 81	1350
	7544/INTELSAT 4-F8	2.0	09 Jan 82	0029
	8985/RB	30.0	06 Jul 81	1717
	12309/COMSTAR	6.9	31 Jul 81	1648
	12309/COMSTAR	6.4	01 Aug 81	1611
	11621/9443	13.5	23 Aug 81	1532
8916/2112 (130°W)	8476/RCA-SATCOM-1	19.0	05 Sep 81	1437
	8476/RCA-SATCOM	46.0	02 Sep 81	1452
	11621/9443	14.0	17 Sep 81	0158
	11621/9443	14.0	18 Sep 81	0153
	8366/GOES-A	2.8	19 Dec 81	0843
	8366/GOES-A	13.0	20 Nov 81	0844
	12089/INTELSAT	7.7	30 Jul 81	0725
	12089/INTELSAT	6.3	30 Jul 81	1929
	12089/INTELSAT-VF-2	3.7	22 Aug 81	1822
	12099/INTELSAT-VF-2	8.0	24 Aug 81	0618
	11669/6393	36.0	20 Sep 81	2113
	11669/6393	33.0	26 Sep 81	2101
	11669/6393	26.0	06 Oct 81	2073
	5854/RB	41.0	13 Nov 81	1333
9785/9364 (20°W)	12089/INTELSAT	7.7	30 Jul 81	0725
	12089/INTELSAT	6.3	30 Jul 81	1929
	12089/INTELSAT-VF-2	3.7	22 Aug 81	1822
	12099/INTELSAT-VF-2	8.0	24 Aug 81	0618
	11669/6393	36.0	20 Sep 81	2113
	11669/6393	33.0	26 Sep 81	2101
	11669/6393	26.0	06 Oct 81	2073
	5854/RB	41.0	13 Nov 81	1333

Table 5 Frequency of encounters for selected geosynchronous satellites ($\Delta T = 30$ days, $R_{MAX} = 500$ km)

Rank	Satellite No.	Satellite name	N_T	\bar{R}_{MIN} , km	V_R , km/s
1	6391	FLTSATCOM	160	203.28	0.06
2	9443	DSCS II	102	358.47	0.12
3	6392	FLTSATCOM	77	178.87	0.08
4	6393	FLTSATCOM	76	332.18	0.10
5	9442	DSCS II	74	289.98	0.18
6	9441	DSCS II	28	291.15	0.10
7	9438	DSCS II	27	302.21	0.12
8	6394	FLTSATCOM D	25	313.63	0.13
9	9434	DSCS II	24	279.17	0.09
10	9444	DSCS II	21	351.29	0.10
11	9363	NATO III-A	20	329.42	0.15
12	9364	NATO III-B	16	315.06	0.13
13	9365	NATO III-C	12	347.59	0.24
14	6395	FLTSATCOM	1	488.69	0.32

Collision Hazards

As an example of the collision hazards in low-altitude orbits, the collision hazard for typical Shuttle missions has been examined via the on-orbit sampling method. A 278-km altitude circular orbit was assumed at 28.5, 57, and 98 deg inclinations.

A set of NORAD catalog objects whose perigee and apogees bracket the Shuttle orbit was selected to determine the number and distribution of close approaches for a typical mission. The results are summarized in Table 1. The results show that the total number of encounters N_T within a 200 km range increases as the inclination increases, the average miss distance \bar{R}_{MIN} is of the order of 145 km, and the average relative velocity is approximately 11 km/s. It can be seen that there are generally more encounters than objects (element sets), indicating that some objects are encountered more than once during the mission.

The normalized relative frequency distribution of encounters for the 28.5-deg inclined orbit is shown in Fig. 6. It can be seen that the relative frequency distribution $f(r)$ can be approximated by a straight line. This approximation can result in an overestimate of the actual collision hazard which may nevertheless be taken as indicative.

Based on geometric considerations, the probability that the Shuttle with an effective collision radius R_s will be hit at encounter is

$$p(\text{col}) = \int_0^{R_s} f(r) dr \quad (2)$$

Since

$$\int_0^{R_{MAX}} f(r) dr = 1 \quad (3)$$

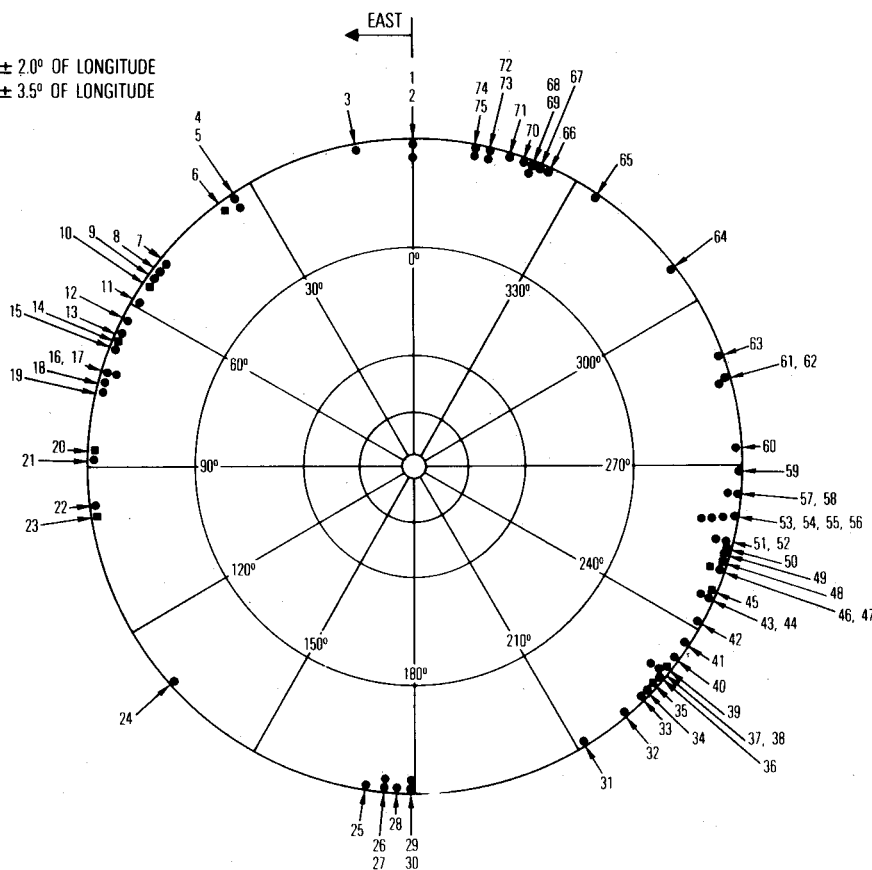


Fig. 7 Geostationary satellites (September 1981-January 1982 NORAD catalog).

and

$$f(r) = CR_{\text{MIN}} \quad (4)$$

where $r = R_{\text{MIN}}$, it follows that

$$C = 2/R_{\text{MAX}}^2 \quad (5)$$

The probability of collision per encounter is

$$p(\text{col}) = 2 \int_0^{R_S} \frac{R_{\text{MIN}}}{R_{\text{MAX}}^2} dR_{\text{MIN}} = \left(\frac{R_S}{R_{\text{MAX}}} \right)^2 \quad (6)$$

and for the mission it is

$$p(\text{col/mission}) = N_T (R_S/R_{\text{MAX}})^2 \quad (7)$$

This result is equivalent to that of Eq. (1) since $f(r)$ was assumed linear. It is equal to the probability of impacting a circular area πR_S^2 within a much larger circular area πR_{MAX}^2 in N_T encounters during a mission, assuming that the probability of impacting the larger area is 1.

For $i = 28.5$ deg, $R_S = 10$ m, $R_{\text{MAX}} = 200$ km, $p(\text{col}/4 \text{ days}) = 0.168$ or $15.3 \times 10^{-6}/\text{yr}$. The collision hazards for the 57 and 98-deg inclination orbits are increased by the ratio of the number of encounters for these orbits. They are 18.0 and $24.7 \times 10^{-6}/\text{yr}$, respectively.

Geosynchronous Orbits

Population

One of the fastest growing satellite groups is at or in the vicinity of the geosynchronous altitude. At these altitudes active satellites maintain fixed longitudinal positions (within a fraction of a degree to several degrees), while inactive spacecraft and debris generally drift around the globe or oscillate about geopotential stable points. A portion of the total geosynchronous population is being tracked by ground stations, while a significant number of smaller objects cannot be seen by radar or optical sensors. A "snapshot" of the

geostationary population (those which remained within ± 2 deg of the nominal longitude between Sept. 20, 1981 and Jan. 21, 1982) is illustrated in Fig. 7 and the objects are listed in Table 2. The locations of all other tracked geosynchronous objects on Sept. 20, 1981 whose drift rates varied from 0.1-5 deg/day are given in Fig. 8 and the objects listed in Table 3.

Distribution of Encounters

Because of the possibility of electromagnetic or physical saturation, the geosynchronous orbit is a limited resource. For example, nominal position and frequency allocations are governed by the provisions of Radio Regulations of the International Telecommunication Union for communication satellites. The actual longitudinal positions of such satellites are generally maintained within ± 1 deg of the nominal position. Several different satellites may, however, share the same general longitudinal location which can result in periodic encounters between spacecraft or between spacecraft and various debris objects. A procedure recently developed by a U.S. government Air Force Satellite Control Facility (AFSCF) monitors all close approaches between a set of primary communication satellites and all other objects that may come within 300 km of these satellites. A prediction is made for all close approaches every seven days, based on numerical integration of appropriate orbits. Appropriate user agencies are alerted at 50 km separation and increased tracking is initiated at 20 km separation. A collision avoidance maneuver is considered at 5-8 km separation and is implemented if near simultaneous tracking of both objects 1-2 days before encounter (closest approach) verifies that the predicted positions of the satellites are accurate. However, a major uncertainty in this procedure is the orbit determination error resulting from inadequate tracking opportunities or other causes. For certain objects the position error can be equal to or greater than the predicted miss distance.

Table 4, for example, shows a distribution of closest approaches for four geosynchronous satellites with the largest number of encounters over a period of six months. It can be

Fig. 8 Nonstationary geosynchronous satellites (September 1981- January 1982 NORAD catalog).

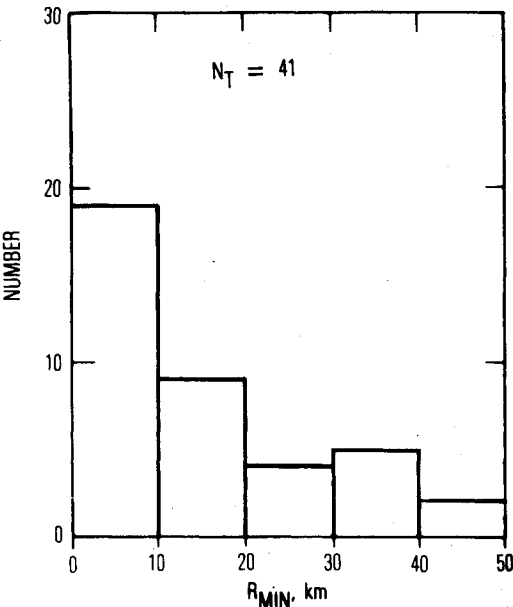
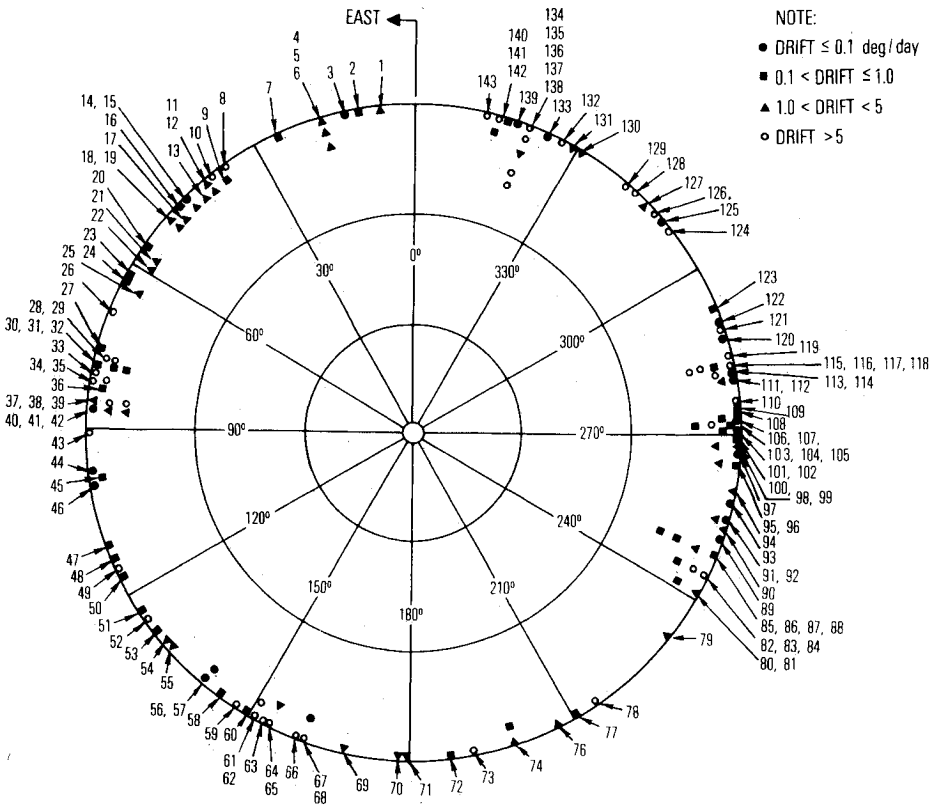


Fig. 9 Four satellite worst case geosynchronous encounter frequency distributions for six months (July 1982-January 1982 NORAD catalog).

seen that several encounters can occur repeatedly if the satellites remain in close proximity to each other over a given period of time. The distribution of the encounters for the four satellites is shown in Fig. 9. A sample of predicted geosynchronous orbit encounters for a satellite located at 240°E longitude is illustrated in Fig. 10. Typical mean relative velocities at encounter are shown in Fig. 11 for satellites at 0 and 240°E longitude as a function of orbital inclination.

Collision Hazard

Frequency of encounters was computed for a number of geosynchronous orbit communication satellites (COMSATS)

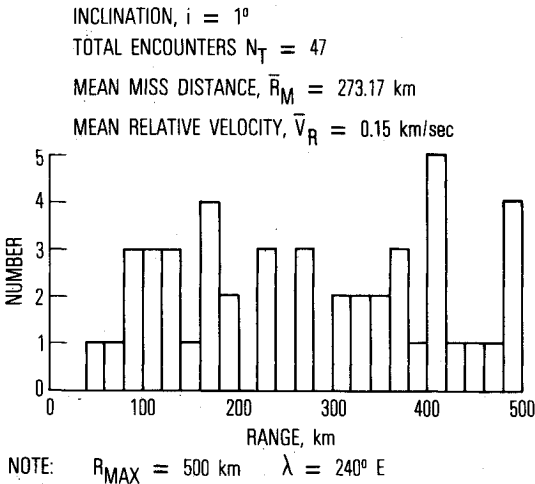


Fig. 10 Sample geosynchronous frequency encounter distribution for 30 days.

as shown in Table 5. The results were obtained by numerical simulation of predicted encounters within 500 km of each satellite for a period of 30 days. The total number of such occurrences varied from 160-1. The mean miss distance and relative velocity for all encounters was also calculated. The encounter frequency N_T differs by about two orders of magnitude depending on the longitudinal location of the primary satellite. Least hazardous orbits may thus be determined by evaluating N_T as a function of the orbital parameters of interest.

For example, the probability of collision for the FLT-SATCOM spacecraft at 100°W longitude can be computed from the encounters listed in Table 4. Since there were seven encounters within 10 km of the spacecraft in six months, Eq. (7) yields $p(\text{col}/6 \text{ months}) = 2.8 \times 10^{-5}$ for an effective collision radius $R_S = 20 \text{ m}$ and $R_{MAX} = 10 \text{ km}$. This is about two orders of magnitude greater than the maximum

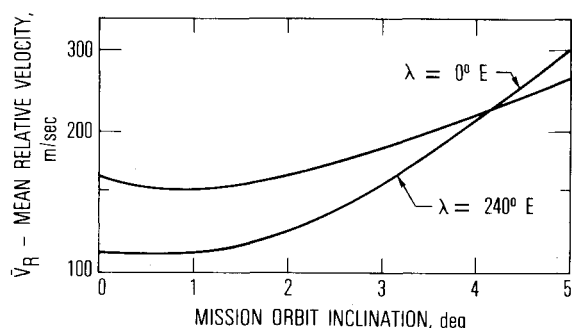


Fig. 11 Sample of relative encounter velocities in geosynchronous orbits.

probability of collision of 4.0×10^{-7} for a "typical" geosynchronous spacecraft based on object density averaged over all longitudes.⁵ The effects of longitudinal bunching of satellites are thus quite significant and should be fully evaluated in assessing the collision hazards for geosynchronous satellites.

Summary and Conclusions

A method of analysis has been described which can be used to determine the probability of collision for a spacecraft in a given orbit. The technique is based on computer sampling of encounter parameters in the vicinity of the mission orbit.

Typical debris flux, relative velocity, and relative angle at encounter were determined for representative circular orbits at different altitudes and orbit plane inclinations. The results show that the flux (and hence the probability of collision) is maximum in the 600-1200 km altitude range for polar and retrograde orbits in general. For the Space Shuttle, the collision probability was found to be of the order of 10^{-5} /yr.

For geosynchronous satellites the effect of orbital concentration (bunching) was found to be significant. For

example, the encounter rate for a number of geostationary COMSATS varied by as much as two orders of magnitude depending on the longitudinal position of the spacecraft. The worst case probability of collision was found to be of the order of 6×10^{-5} /yr, some two orders of magnitude greater than that for a "typical" geosynchronous satellite.

In view of the results presented it can be concluded that the probability of collision for a spacecraft in orbit is a function of altitude and orbit plane inclination, as well as longitudinal position for geostationary satellites. The described method of analysis can be used effectively to determine these dependencies.

Acknowledgment

This work reflects research conducted under U.S. Air Force Space Division Contract F04701-82-C-0083.

References

- ¹Kessler, D.J., "Sources of Orbital Debris and Projected Environment for Future Spacecraft," *Journal of Spacecraft and Rockets*, Vol. 18, July-Aug. 1981, p. 357.
- ²Hechler, M. and Van der Ha, J.C., "Probability of Collisions in the Geostationary Ring," *Journal of Spacecraft and Rockets*, Vol. 18, July-Aug. 1981, p. 361.
- ³Sehnal, L. and Pospisilova, L., "Collisions of Artificial Earth Orbiting Bodies," *Bulletin of the Astronautical Institute of Czechoslovakia*, Vol. 32, 1981, pp. 310-315.
- ⁴Chobotov, V.A., "Collision Hazard in Space," *Astronautics & Aeronautics*, Vol. 18, No. 9, Sept. 1981, pp. 38-39.
- ⁵Chobotov, V.A., "The Collision Hazard in Space," *Journal of Astronautical Sciences*, Vol. XXX, No. 3, July-Sept. 1982, p. 191.
- ⁶Reynolds, R.C., Fisher, N.H. and Rice, E.E., "Man-Made Debris in Low Earth Orbit—A Threat to Future Operations," *Journal of Spacecraft and Rockets*, Vol. 20, No. 3, May-June 1983, pp. 279-285.

From the AIAA Progress in Astronautics and Aeronautics Series...

ELECTRIC PROPULSION AND ITS APPLICATIONS TO SPACE MISSIONS—v. 79

Edited by Robert C. Finke, NASA Lewis Research Center

Jet propulsion powered by electric energy instead of chemical energy, as in the usual rocket systems, offers one very important advantage in that the amount of energy that can be imparted to a unit mass of propellant is not limited by known heats of reaction. It is a well-established fact that electrified gas particles can be accelerated to speeds close to that of light. In practice, however, there are limitations with respect to the sources of electric power and with respect to the design of the thruster itself, but enormous strides have been made in reaching the goals of high jet velocity (low specific fuel consumption) and in reducing the concepts to practical systems. The present volume covers much of this development, including all of the prominent forms of electric jet propulsion and the power sources as well. It includes also extensive analyses of United States and European development programs and various missions to which electric propulsion has been and is being applied. It is the very nature of the subject that it is attractive as a field of research and development to physicists and electronics specialists, as well as to fluid dynamicists and spacecraft engineers. This book is recommended as an important and worthwhile contribution to the literature on electric propulsion and its use for spacecraft propulsion and flight control.

888 pp., 6 × 9, illus., \$30.00 Mem., \$55.00 List

TO ORDER WRITE: Publications Order Dept., AIAA, 1633 Broadway, New York, N.Y. 10019